Behavior of a liquid drop in a rounded corner: Different contact angles

Cite as: AIP Advances **9**, 085203 (2019); https://doi.org/10.1063/1.5100300
Submitted: 16 April 2019 . Accepted: 24 July 2019 . Published Online: 05 August 2019

Zhiyi Han (韩志一), Li Duan (段俐), and Qi Kang (康琦)

Behavior of a liquid drop in a rounded corner: Different contact angles

Cite as: AIP Advances 9, 085203 (2019); doi: 10.1063/1.5100300
Submitted: 16 April 2019 • Accepted: 24 July 2019 •
Published Online: 5 August 2019

View Online Export Citation CrossMark

Zhiyi Han (韩志一),[1,2] Li Duan (段俐),[1,2,a)] and Qi Kang (康琦)[1,2]

AFFILIATIONS

[1]Key Laboratory of Microgravity, Institute of Mechanics, Chinese Academy of Sciences, No. 15 Beisihuanxi Road, Beijing, 100190, China
[2]School of Engineering Science, University of Chinese Academy of Sciences, No. 19(A) Yuquan Road, Shijingshan District, Beijing, 100049, China

[a)]**Corresponding author e-mail address:** duanli@imech.ac.cn

ABSTRACT

The Concus-Finn condition, based on the local microscopic contact angle, can be used to predict discontinuous behavior of a liquid drop in an ideally sharp corner. However, since ideally sharp corners do not exist in reality, it is important to understand the effect of rounded corners on the behavior of liquid drops. In this paper, we use theoretical calculations to study the behavior of two-dimensional liquid drops in rounded corners, including the case in which the contact angles on the two sides of the corner may differ. A new discontinuous behavior was discovered in our study, which is different from the case in sharp corners. Comparing the situation in sharp corners, our study shows that the behavior of a drop in a rounded corner depends on the dimensionless volume of the drop, in addition to its dependence on the opening angle and contact angles that is covered by the Concus-Finn condition. We also use energy-minimization approach to successfully explain why this discontinuous behavior occurs in rounded corners.

I. INTRODUCTION

Wetting behavior is a field at the intersection of fluid mechanics, statistical physics and physical chemistry.[1,2] It plays an important role in a variety of applied processes such as the control of fluid transport,[3] the design of devices for filtering or sensing,[4] industrial coatings,[5] and designing biomimetic superhydrophobic surface.[6] Fine details of the wetting behavior of a nano-drop can be obtained by using molecular dynamics simulation.[7,8] The wetting process on a solid surface has also supplied researchers with a valuable model system to study a number of interesting fluid problem.[9–13] Also, shape reconfiguration is central to emerging applications that exploit the physics of liquids confined by surface tension on the microscale. Surface tension largely determines the surface shape on scales smaller than the capillary length. In space applications, the capillary length for a liquid against vapor can be 100cm, whereas it is usually a few millimeters on Earth.[14]

Interior corners are common constructs employed in spacecraft fluids systems to passively control large length scale capillary-dominated liquid in a desired manner.[15,16] The behaviors of a liquid drop in a sharp corner have been previously explored by Concus and Finn, together with their collaborator[17–21] (see Ref. 20 or Ref. 21, for example, for a summary of their works). And the Concus-Finn condition can be used to determine the behavior of the droplet in the corner, based on the local microscopic contact angle, which can then be used to determine optimal angle to promote liquid management.[22] The equilibrium morphology and position of a liquid drop inside a corner under different wettability conditions has been studied analytically,[23] numerically[20] and experimentally,[24] which shows the shape of the drop in a corner is a portion of a sphere.

The Concus-Finn condition firstly published by Concus and Finn[17] states that the surface of the liquid drop in a sharp corner with opening angle 2α is unbounded for:

$$\alpha + \theta < \frac{\pi}{2} \tag{1}$$

where θ is the contact angle. In other words, there is no equilibrium free surface of liquid drop existing for this condition given by Eq. (1). For the case where $\alpha + \theta > \pi/2$, there exists an equilibrium free surface in a sharp corner. Several years later, Concus and Finn applied

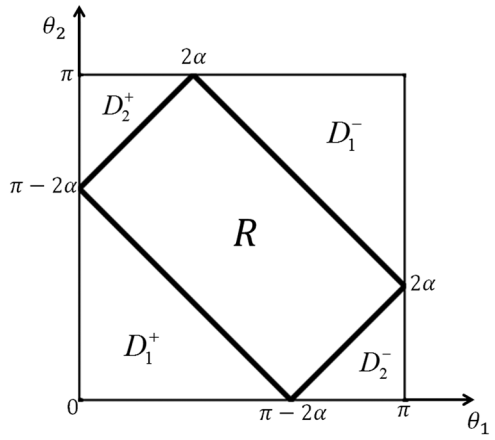

FIG. 1. The Concus-Finn diagram (modified from[19,21]): regions in parameter space corresponding to different behaviors at a sharp corner with opening angle 2α.

their earlier derivations to a corner region for the case in which the contact angles on the two sides of the corner have different values.[19] New boundary conditions were developed that incorporate the difference in contact angle between the two solid surfaces of the corner. These conditions were represented graphically as seen in Fig. 1. In this figure, the horizontal axis and the vertical axis represent the values of the contact angle for each surface, θ_1 and θ_2, respectively. The rectangle R in the θ_1-θ_2 plane cuts off triangular regions D_1^+, D_1^-, D_2^+, D_2^- in the $\pi \times \pi$ square, as indicated. For the points lying in the region R, which is inclined across the square $\pi \times \pi$ area where $\pi - 2\alpha < \theta_1 + \theta_2 < \pi + 2\alpha$ and $|\theta_1 - \theta_2| < \pi - 2\alpha$, the liquid drop is a blob in the shape of a portion of a sphere in contact with the edge (the vertex of the sharp corner). For the points lying in the region of D_1^+ where $\theta_1 + \theta_2 < \pi - 2\alpha$, the liquid drop can't remain as a blob in the edge and will spread arbitrarily far along the edge (spread out to infinity in the edge). For the points lying in the region of D_1^- where $\theta_1 + \theta_2 > \pi + 2\alpha$, the liquid drop forms a spherical bridge. By the way, Luo *et al.*[25] have got the same result during investigating a stable intermediate wetting state of a water drop being placed on a corner. For the points lying in the region of D_2^+ where $\theta_2 - \theta_1 > \pi - 2\alpha$ and D_2^- where $\theta_1 - \theta_2 < \pi - 2\alpha$, the drop forms a spherical cap contacting only one of the solid surfaces (resting on a single surface) of the sharp corner and the another solid surface being contacted in a vacuous sense.[21] Those phenomena can be illustrated by some representative configurations in Fig. 2.

The Concus-Finn condition is universal for various system geometries, providing they have ideally sharp corners. And the behavior of a liquid drop in a sharper corner has been studied extensively, including the dynamics of drop migration,[26–28] the effect of contact angle hysteresis[29–36] and wetting or dewetting behavior in corners.[37,38] However, due to either design or fabrication, the interior corners are not perfectly sharp but rather possess a degree of roundedness. Also, the impact of corner imperfections such as corner roundedness has not been fully characterized analytically.[15] Actually, even slight roundedness can prevent the spreading of liquid drops in otherwise wettable corners, so it is critical to systematically and quantitatively analyze the impact of the degree of roundedness on wetting behavior.

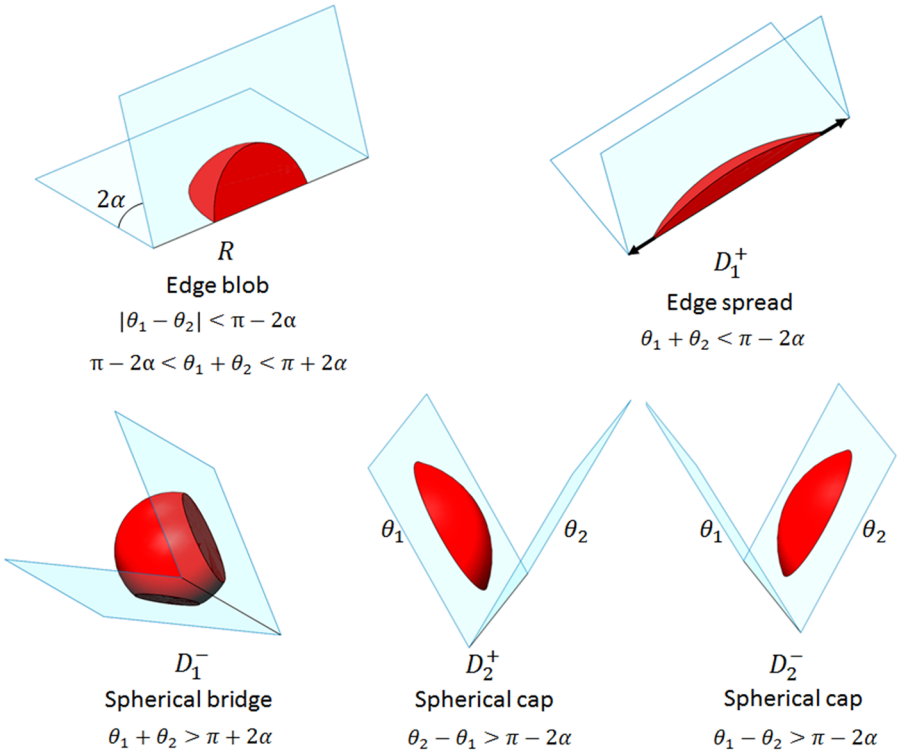

FIG. 2. Representative configurations for varying contact angle data (modified from[20,21]).

The behavior of a liquid drop in a rounded corner has been explored preliminarily in the case of $\theta < \pi/2 - \alpha$, which shows that the spreading of the drop stops at a finite length and does not proceed indefinitely.[39] And the spreading of the droplet is strongly influenced by the smoothness of the corner.[40]

In this paper we focus on the behavior for equilibrium configurations of liquid drops in rounded corners considering that the contact angle varies from 0 to π, including the case when the contact angles on the two sides of the corner are different. Our goal is to illustrate the behavior of a drop in a rounded corner by using relevant examples to show the differences and connections between the situation in a rounded corner and in a sharp corner. In addition, our study focuses on two-dimensional drops due to the complexity of the equilibrium morphology of three-dimensional drops exposed to rounded corners. There are still many wetting phenomena in some two-dimensional structures.[23,41,42] The restriction to 2D simplifies the problem and is the first step towards understanding the influence of spatial situation.

II. BEHAVIOR OF A DROP IN A ROUNDED CORNER

A. Discontinuous behavior of a 2D drop in a rounded corner

Small changes in contact angle, geometry or volume of the drop can result in large changes, possibly discontinuous, of the equilibrium fluid configuration, which is called discontinuous behavior.[20] The gravity is absent or can be neglected, which is the situation we discuss here. Based on the classical Young equation for an equilibrium free surface of a liquid drop in contact with solid support surfaces, a new discontinuous behavior has been discovered in our work.

As illustrated in Fig. 3, for simplicity, a rounded corner is defined by a circle of radius r that is smoothly connected to the walls of the corner (the walls are tangent to the circle at the connection point). We use solid surface 1 and solid surface 2, respectively, to denote the left side solid surfaces and right side solid surfaces of the rounded corner. The solid surface 1 (blue) consists of straight wall 1 and rounded wall 1. Also, the solid surface 2 (red) consists of straight wall 2 and rounded wall 2. We let θ_1 represent the equilibrium contact angle on the solid surface 1 and use θ_2 to stand for the one on the solid surface 2. In addition, we assume that the walls are isotropic, smooth substrates without hysteresis.

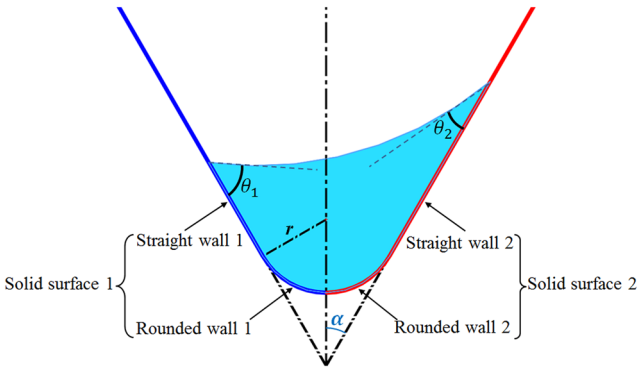

FIG. 3. A rounded corner with two different substrates (two different solid surfaces), which consist of straight walls and rounded walls. The rounded walls smoothly connected to the straight walls.

The interfacial energy of the system, E, is given by

$$E = \sigma S_{lv} + (\sigma_{sl1} - \sigma_{sv1})S_{sl1} + (\sigma_{sl2} - \sigma_{sv2})S_{sl2} \tag{2}$$

In this equation, we let σ_{sl1} represent solid-liquid interfacial tension on the solid surface 1 and use σ_{sl2} stand for the one on the solid surface 2. Also, we use σ_{sv1} and σ_{sl2} to represent the solid-vapor surface tension of these two solid surfaces, respectively. And S_{sl1} and S_{sl2} are the solid-liquid interfacial areas of these two solid surfaces, respectively. Additionally, σ and S_{lv} are liquid-vapor surface tension and area of the liquid-vapor free surface, respectively.

A stable equilibrium configuration occurs when the interfacial energy E minimizes, under the condition of fixed liquid volume V. The volume V enclosed by the capillary surface is held constant:

$$V[\mathrm{x}] \equiv \int_V \mathrm{d}V = \mathrm{C} \tag{3}$$

We can treat the volume-conservation constraint as an auxiliary condition by introducing the Lagrange multiplier μ into an augmented functional,

$$F[x] = E[x] - \mu \cdot V[x] \tag{4}$$

The surface equilibrium conditions arise from the first variation of the energy functional. The first variation of the augmented functional to be zero $\delta F = 0$ is the same as the one of the energy functional $\delta E = 0$ because of the volume-conservation constraint $\delta V = 0$. The equilibrium condition requiring $\delta E = 0$, but to obtain the stability condition we also need $\delta^2 E > 0$. The equilibrium free surfaces so determined are surfaces of constant mean curvature meeting the solid surfaces with contact angle. Usually, these free surfaces of liquid drops exposed to rounded corner constraints in three dimensional space are very complex. But in two dimensions, it is possible to derive an analytical expression of the energy minimum. We note that at given fixed liquid volume, a plethora of solutions exists, each formed with liquid-vapor interfaces having constant curvature – that is, a simple circular arc, in the plane – satisfying the Young equation at the solid surfaces. In this 2D geometry, discontinuous behavior occurs when $|\theta_1 - \theta_2|$ exceeds a critical value. Fig. 4 is a special example to show this discontinuous change in behavior. As illustrated in Fig. 4(a), a tiny change in θ_1 results in a tiny change of the equilibrium configuration if $|\theta_1 - \theta_2|$ doesn't exceed a critical value, which is called continuous behavior. Otherwise, a tiny change in θ_1 results in a large change of the equilibrium configuration if $|\theta_1 - \theta_2|$ exceeds a critical value, which is also means discontinuous behavior, as illustrated in Fig. 4(b). Finally, the drop only contacts the solid surface 2 and the solid surface 1 is contacted in a vacuous sense.

B. Liquid bridge in a rounded corner

We also found conditions under which an equilibrium circular bridge in a 2D rounded corner would be possible in zero gravity (Fig. 5). The shape of the drop is a truncated disk. To maintain a liquid bridge with circular morphology, the drop should only contact the straight walls, not the rounded walls. Once the drop contacts the rounded walls, the liquid bridge with circular morphology cannot

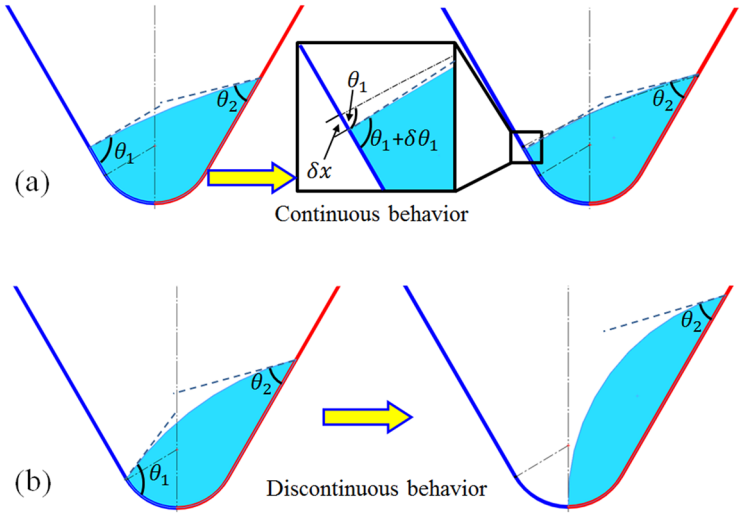

FIG. 4. (a) Continuous behavior: a tiny increment of $\theta_1(\delta\theta_1)$, results in a tiny displacement of contact line (δx). (b) Discontinuous behavior: a tiny increment of θ_1 results in a large displacement of contact line.

exist. We assume that the radius of the truncated disk in Fig. 5 is R. The volume V of the drop confined between the straight walls is:

$$V = (\theta_1 + \theta_2 - \pi - \sin\theta_1\cos\theta_1 - \sin\theta_2\cos\theta_2)R^2 \tag{5}$$

To maintain an equilibrium liquid bridge in a rounded corner, the drop only contacts the straight walls, not contacts the rounded walls, which means the geometrical relationships in Fig. 5 must be satisfied. We have:

$$r\cot\alpha + R\sin\theta_2 < -R\cos\theta_2\cot\alpha_2 \tag{6}$$

because

$$\alpha_1 + \alpha_2 = 2\alpha \tag{7}$$

$$\sin\alpha_1 = \frac{-R\cos\theta_1}{l} \tag{8}$$

$$\sin\alpha_1 = \frac{-R\cos\theta_2}{l} \tag{9}$$

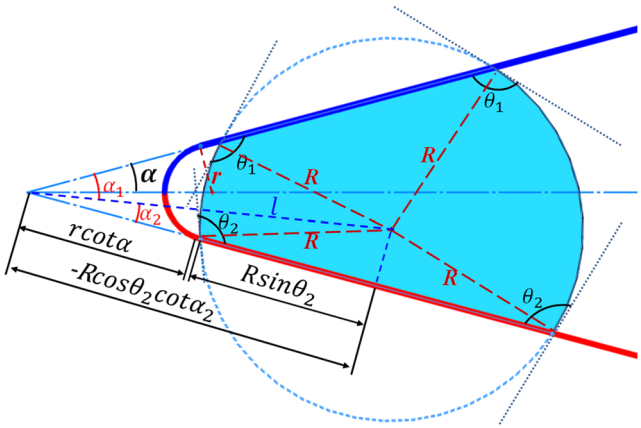

FIG. 5. An equilibrium liquid bridge in a rounded corner. The drop only contacts the straight walls, not contacts the rounded walls.

So we get:

$$\cot\alpha_2 = \frac{\cos\theta_1 + \cos\theta_2\cos 2\alpha}{\cos\theta_2\sin 2\alpha} \tag{10}$$

Substitute Eq. (10) into Eq. (6) and we have:

$$\frac{R}{r} > -\frac{2\cos^2\alpha}{\cos\theta_1 + \cos\theta_2\cos 2\alpha + \sin\theta_2\sin 2\alpha} \tag{11}$$

Substitute Eq. (11) into Eq. (5) and we have:

$$V \geq (\theta_1+\theta_2 - \pi - \sin\theta_1\cos\theta_1 - \sin\theta_2\cos\theta_2) \times \left[\frac{2\cos^2\alpha}{\cos\theta_1 + \cos\theta_2\cos 2\alpha + \sin\theta_2\sin 2\alpha}\right]^2 r^2 \tag{12}$$

Which is the condition to maintain an equilibrium circular bridge in a 2D rounded corner.

By the way, in 3D space, the shape of the drop is a truncated sphere because the spherical morphology is only possible if the drop can maintain a stable liquid bridge in a corner.[20,23] Similarly, to maintain an equilibrium spherical bridge in a 3D rounded corner also requires the drop only contacting straight walls. The corresponding condition becomes:

$$V \geq \frac{\pi}{3}(\cos^3\theta_1 - 3\cos\theta_1 + \cos^3\theta_2 - 3\cos\theta_2) \times \left[\frac{2\cos^2\alpha}{-\cos\theta_1 - \cos\theta_2\cos 2\alpha - \sin\theta_2\sin 2\alpha}\right]^3 r^3 \tag{13}$$

If the volume V tends to infinity, both Eq. (12) and Eq. (13) will be reduced to $\theta_1 + \theta_2 > \pi + 2\alpha$, which is also the condition to form a stable liquid bridge in a sharp corner.[19,21]

C. Boundary conditions of regions in $\pi \times \pi$ square

The behavior of a drop in a rounded corner depends on the radius of rounded corner and on the volume of the drop, in addition to its dependence on the opening angle and contact angles that is covered by the Concus-Finn condition.[39] In two dimensions, in order to decrease the number of parameters in the Eq. (2),

the dimensionless volume of drop is defined as $V^* = V/r^2$. And the dimensionless interfacial energy, E^*, defined by the following equation, will be used

$$E^* = \frac{E}{\sigma r} = S_{lv}^* - S_{sl1}^* \cos\theta_1 - S_{sl2}^* \cos\theta_2 \tag{14}$$

Where $S_{lv}^* = S_{lv}/r$, $S_{sl1}^* = S_{sl1}/r$, $S_{sl2}^* = S_{sl2}/r$, $\cos\theta_1 = (\sigma_{sv1} - \sigma_{sl1})/\sigma$ and $\cos\theta_2 = (\sigma_{sv2} - \sigma_{sl2})/\sigma$, by the Young equation. Theoretical results of drop position and morphology can be obtained by minimizing E^* under the condition of fixed drop volume V^*. Combined with the conditions for forming the liquid bridge in a rounded

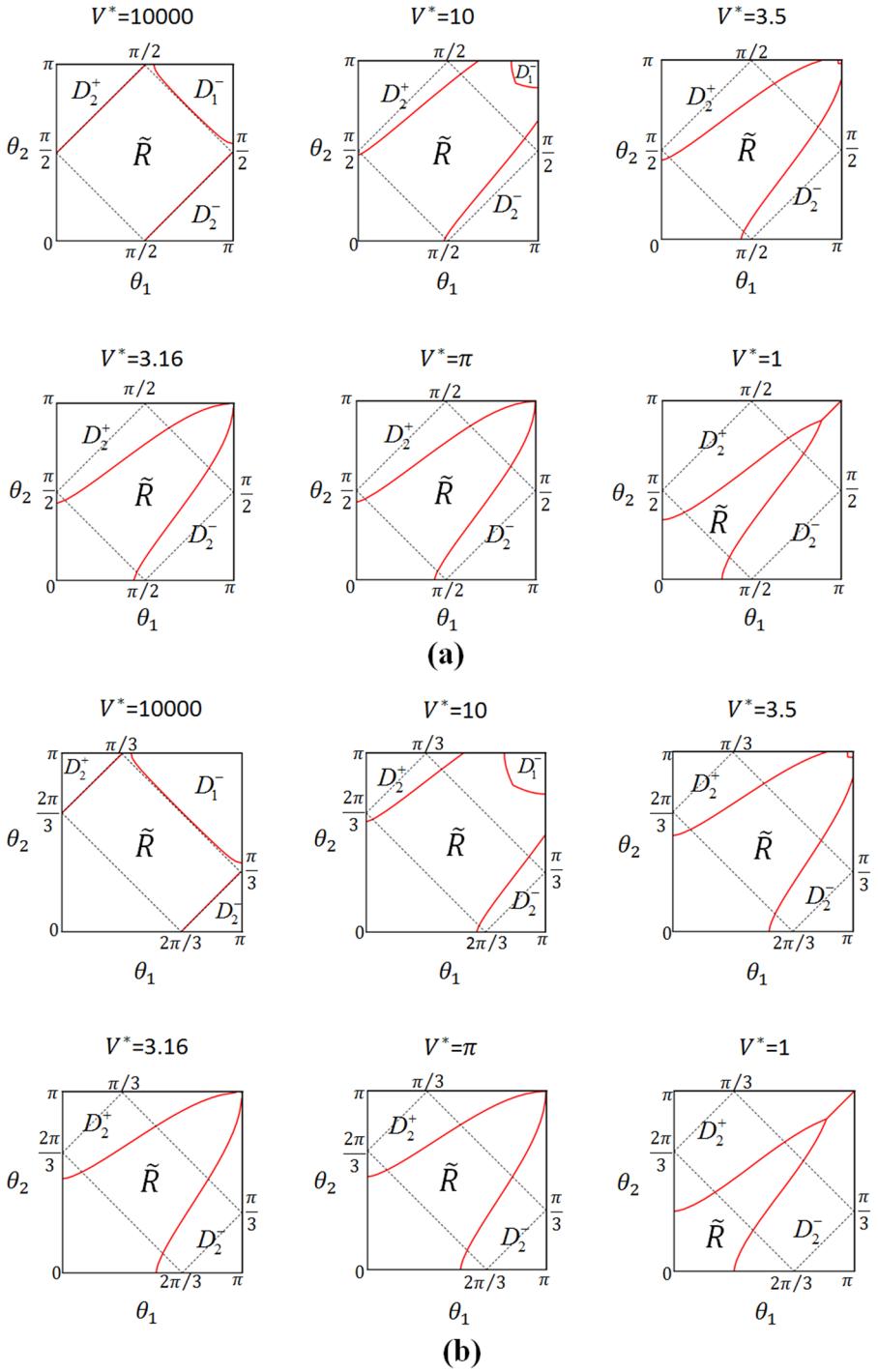

FIG. 6. Regions in parameter space corresponding to different behaviors at a rounded corner with opening angle 2α and dimensionless volume V^*. (a) $\alpha = \pi/4$; (b) $\alpha = \pi/3$. The dimensionless volume $V^* = 10000, 10, 3.5, \pi, 1$. The black dashed lines in every parameter space represent Concus-Finn condition, just like the thick solid lines in Fig. 1. And the red solid lines represent boundary conditions of different behaviors in a rounded corner.

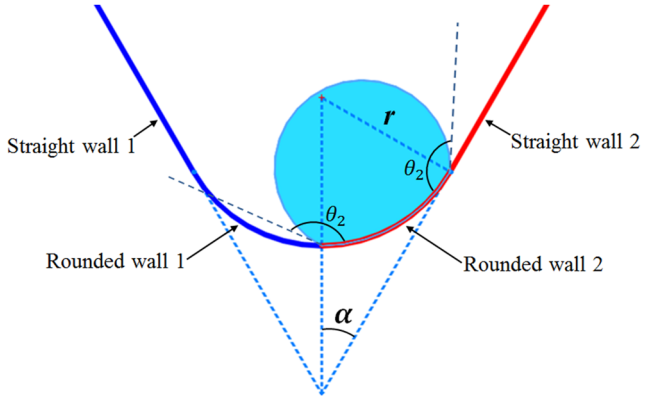

FIG. 7. Limiting configuration of D_2^- when $V^* = 1$, $\theta_1 > \theta_2 = 152.46°$, the drop only contacts the rounded wall 2.

corner (Eq. (12)), we can get new boundary conditions about different behaviors, which is represented graphically as seen in Fig. 6.

The results in Fig. 6 are very different from the results in Fig. 1. We use $\tilde{R}$ instead of R because the region $\tilde{R}$ in Fig. 6 is no longer a rectangle. From Fig. 6, we can see when the dimensionless volume of the drop is very large, for example, $V^* = 10000$, the behavior of the drop in rounded corner is similar to the one in sharp corner, except there is no region of D_1^+ because only in the case $\theta_1 = 0$ or $\theta_2 = 0$ will the drop spread indefinitely along a rounded corner. We can also image if $V^* \to \infty$, the boundary conditions of different behaviors are reduced to the Concus-Finn condition. With the decrease of V^*, the region D_1^- is shrunk and the regions D_2^+, D_2^- are enlarged. The regions D_2^+, D_2^- in Fig. 6 indicates that discontinuous behavior occurs since $|\theta_1 - \theta_2|$ exceeds a critical value, as illustrated in Fig. 4(b). In a sharp corner, this critical value is $\pi - 2\alpha$, which is one of results that Concus-Finn has already got[21] as aforementioned in Section I. But in a rounded corner, this critical value depends not only on the opening angle 2α, θ_1 and θ_2, but also on the dimensionless volume V^*. The region D_1^- will disappear when V^* decreases to π. If $V^* < \pi$, for example, $V^* = 1$, the regions D_2^+, D_2^- are further enlarged and they border each other, as shown the last graph in Fig. 6(a) and Fig. 6(b). This is because when θ_1 or θ_2 is sufficiently large, a tiny difference between θ_1 and θ_2 can cause the little drop to contact only one solid surface of the corner. An example of these drop configurations is shown in Fig. 7. Strictly speaking, the drop only contacts the rounded wall 2.

III. ENERGY PROFILES

We can compute directly the extremum of interfacial energy at a given droplet volume, opening angle and contact angles for a rounded corner. Sometimes we can only get a minimum of E^* when $\delta E^* = 0$. And sometimes we can obtain three extrema of E^* when $\delta E^* = 0$, which means there are triple equilibrium states. In these three extrema of interfacial energy, two of them are minimums ($\delta^2 E > 0$) and one is maxima ($\delta^2 E < 0$). Otherwise, only one minimum of interfacial energy can be obtained. Fig. 8 shows a special example of drop configurations when three extrema can be obtained.

All configurations in Fig. 8 meet contact angle conditions and have constant mean curvature surfaces, which means they all satisfy

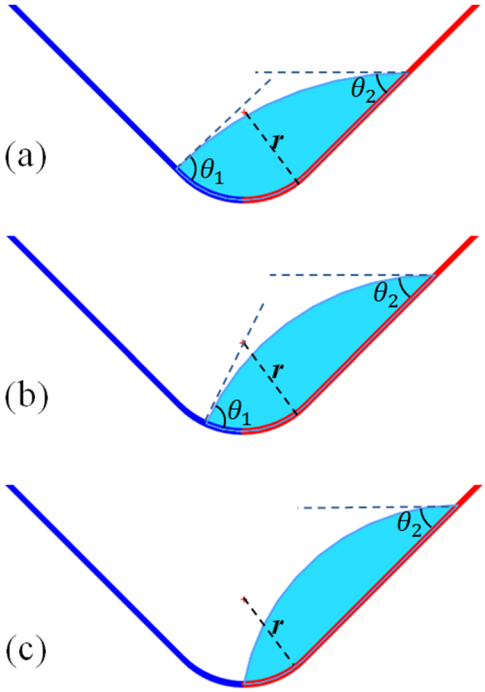

FIG. 8. Three equilibrium configurations: (a) A stable equilibrium configuration with minimum of energy. (b) An unstable equilibrium configuration with maxima of energy. (c) A stable equilibrium configuration with minimum of energy.

the local balance of forces. Fig. 8(a) illustrates a stable equilibrium position of the drop when the energy minimum is obtained. We can see that the contact line on the left is on the straight wall 1. Fig. 8(b) illustrates an unstable equilibrium position when the energy maximum is obtained. We can see that the contact line on the left is on the rounded wall 1. Fig. 8(c) illustrates another stable equilibrium position when the other energy minimum is obtained. We can see that the contact line on the left is at the boundary between rounded wall 1 and rounded wall 2, therefore the drop only contacts the solid wall 2. Both configurations in Fig. 8(a) and Fig. 8(c) correspond to a stable equilibrium. Between these two positions, there exists an unstable equilibrium (Fig. 8(b)) with a maximum of energy. Both the energetic approach and the one based on the balance of forces show that sometimes a rounded corner wall can result in triple equilibrium states.

We investigate the energy profile numerically for a given fixed volume and opening angle as a function of θ_1 (or θ_2) to indicate that there is a region where three extrema exist as illustrated in Fig. 9. And we can see the *Energy minimum 1* monotonically increases with θ_1 until θ_1 reaches a critical value (in Fig. 9, this critical value is 105.75°) where the energy is discontinues and decrease suddenly. Beyond this value, the energy is constant. In fact, discontinues behavior occurs when θ_1 exceeds this value. Since θ_2 is constant in Fig. 9, we can assert that discontinues behavior occurs if $|\theta_1 - \theta_2|$ exceeds a critical value just as same as the one aforementioned in Section II. Now we can say that discontinuous behavior is accompanied by discontinuous changes in energy while continuous behavior is accompanied by continuous changes in energy. If θ_1 is

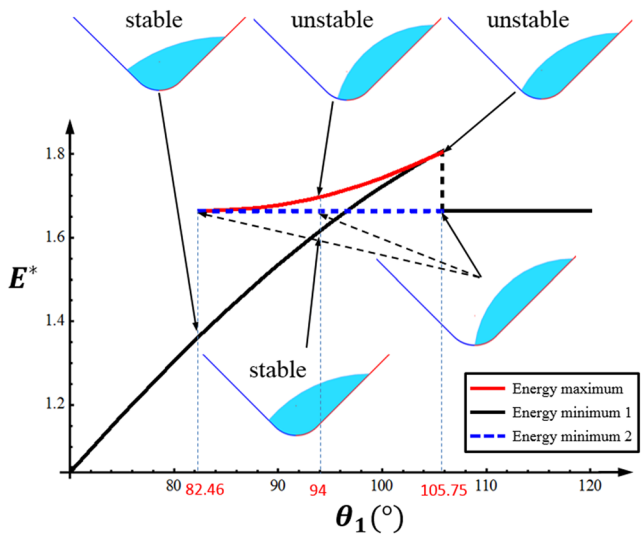

FIG. 9. Total interfacial energy E^* as a function of θ_1, for a given $\theta_2 = 45°$, $\alpha = 45°$, $V^* = \pi$. If $82.46° < \theta_1 < 105.75°$, there are three extrema (Energy minimum 1, Energy minimum 2 and Energy maximum). Otherwise, only Energy minimum 1 exists.

below a certain value (in Fig. 9, this certain value is 82.46°), there is only one equilibrium state where the *Energy minimum 1* is reached. In addition, *Energy minimum 2* represents another stable state where the drop only contacts the solid wall 2 as illustrated in Fig. 8(c), and *Energy maximum* represents an unstable state where the contact line on the left is on the rounded wall 1 as illustrated in Fig. 8(b).

We now consider the case in which the opening angle is variable for a given fixed volume, θ_1 and θ_2. From the energy profile numerically plotted in Fig. 10, we see that there is still a region

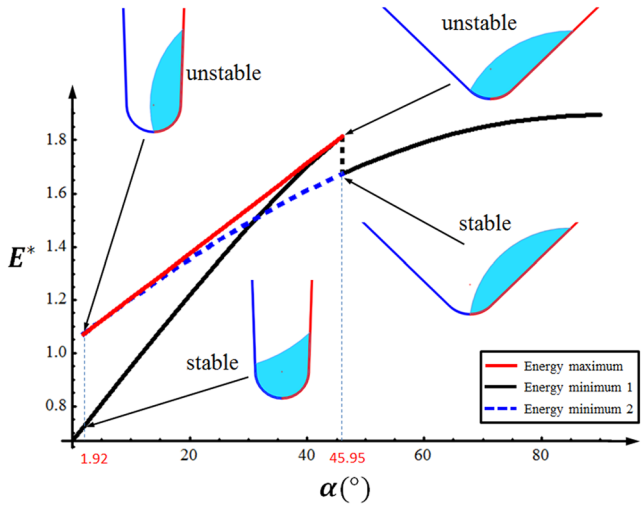

FIG. 10. Total interfacial energy E^* as a function of α, for a given $\theta_1 = 105°$, $\theta_2 = 45°$, $V^* = \pi$, If $1.92° < \theta_1 < 45.95°$, there are three extrema (Energy minimum 1, Energy minimum 2 and Energy maximum). Otherwise, only Energy minimum 1 exists.

where three extrema exist. There is also a critical value (in Fig. 10, this critical value is 45.95°) of α where the energy is discontinues and decrease suddenly. The energy increases monotonically with α except at this critical value. Discontinues behavior occurs when α exceeds this critical value. Similar to the case in Fig. 9, if α is below a certain value (in Fig. 10, this certain value is 1.92°), there is only one equilibrium state where the *Energy minimum 1* is reached. From the previous discussion, it can be concluded that discontinuous behavior is accompanied by a sudden decrease in energy.

IV. CONCLUSION

In this work, we have used theoretical calculations, dimensional analysis to study the behavior of two-dimensional liquid drops in rounded corners for the case in which the contact angles on the two sides of the corner have different values. A new discontinuous behavior was discovered in our study, which is very different from the case in sharp corners. Comparing the situation in sharp corners, our study shows that the behavior of a drop strongly depends on the radius of rounded corners and the volume of the drop, in addition to its dependence on the opening angle and contact angles that is covered by the Concus-Finn condition. Furthermore, we found that discontinuous behavior is accompanied by a sudden decrease in energy through the energy-minimization approach. Continuous changes in energy result in continuous behavior, while discontinuous changes in energy lead to discontinuous behavior. We now have a thorough physical picture of how geometrical and volumetric parameters affect the behavior of liquid drop in two dimensions. The two-dimensional results could help us to study the three-dimensional situation in further work. We hope the outcome of this work will motivate further analytical and experimental studies on the behavior of liquids coupled with geometric constraints, for developing applications in space liquid management or in microfluidics.

ACKNOWLEDGMENTS

This research was supported by the China Manned Space Engineering program (Fluid Physics Experimental Rack), the National Natural Science Foundation of China (U1738116).

REFERENCES

[1] D. Bonn, J. Eggers, J. Indekeu, J. Meunier, and E. Rolley, "Wetting and spreading," Rev. Mod. Phys. **81**(2), 739–805 (2009).
[2] P. G. de Gennes, "Wetting: Statics and dynamics," Rev. Mod. Phys. **57**(3), 827–863 (1985).
[3] J. Y. Huang, Y.-C. Lo, J. J. Niu, A. Kushima, X. Qian, L. Zhong, S. X. Mao, and J. Li, "Nanowire liquid pumps," Nat. Nanotech. **8**, 277–281 (2013).
[4] T. M. Squires and S. R. Quake, "Microfluidics: Fluid physics at the nanoliter scale," Rev. Mod. Phys. **77**, 977–1026 (2005).
[5] Y. Pomeau and E. Villermaux, "Two hundred years of capillarity research," Phys. Today **59**(3), 39–44 (2006).
[6] A. Tuteja, W. Choi, M. Ma, J. M. Mabry, S. A. Mazzella, G. C. Rutledge, G. H. McKinley, and R. E. Cohen, "Designing superoleophobic surfaces," Science **318**(5856), 1618–1622 (2007).
[7] M. Foroutan, S. M. Fatemi, F. Esmaeilian, V. F. Naeini, and M. Baniassadi, "Contact angle hysteresis and motion behaviors of a water nano-droplet on suspended graphene under temperature gradient," Phys. Fluids **30**(5), 052101 (2018).
[8] Q. Yuan and Y. P. Zhao, "Topology-dominated dynamic wetting of the precursor chain in a hydrophilic interior corner," Proc. R. Soc. A **468**(2138), 310–322 (2011).

[9]S. Herminghaus, M. Brinkmann, and R. Seemann, "Wetting and dewetting of complex surface geometries," Annu. Rev. Mater. Res. **38**(1), 101–121 (2008).
[10]D. Peschka, "Variational approach to dynamic contact angles for thin films," Phys. Fluids **30**(8), 082115 (2018).
[11]F.-C. Yang, X.-P. Chen, and P. Yue, "Surface roughness effects on contact line motion with small capillary number," Phys. Fluids **30**(1), 012106 (2018).
[12]T. Omori and T. Kajishima, "Apparent and microscopic dynamic contact angles in confined flows," Phys. Fluids **29**(11), 112107 (2017).
[13]A. R. Harikrishnan, P. Dhar, P. K. Agnihotri, S. Gedupudi, and S. K. Das, "Correlating contact line capillarity and dynamic contact angle hysteresis in surfactant-nanoparticle based complex fluids," Phys. Fluids **30**(4), 042006 (2018).
[14]J. B. Bostwick and P. H. Steen, "Stability of constrained capillary surfaces," Annu. Rev. Fluid Mech. **47**(1), 539–568 (2015).
[15]Y. K. Chen, M. M. Weislogel, and C. L. Nardin, "Capillary-driven flows along rounded interior corners," J. Fluid Mech. **566**, 235–271 (2006).
[16]M. M. Weislogel, "Capillary flow in interior corners: The infinite column," Phys. Fluids **13**, 3101 (2001).
[17]P. Concus and R. Finn, "On the behavior of a capillary surface in a wedge," Proc. Natl. Acad. Sci. U. S. A. **63**, 292–299 (1969).
[18]P. Concus and R. Finn, "On capillary free surfaces in the absence of gravity," Acta Math. **132**(1), 177–198 (1974).
[19]P. Concus and R. Finn, "Capillary surfaces in a wedge: Differing contact angles," Microgravity Sci. Tech. **7**, 152–155 (1994).
[20]P. Concus and R. Finn, "Discontinuous behavior of liquids between parallel and tilted plates," Phys. Fluids **10**, 39–43 (1998).
[21]P. Concus, R. Finn, and J. McCuan, "Liquid bridges, edge blobs, and Scherk-type capillary surfaces," Indiana Univ. Math. J. **50**, 411–441 (2001).
[22]C. D. Rath and S. G. Kandlikar, "Liquid filling in a corner with a fibrous wall–An application to two-phase flow in PEM fuel cell gas channels," Colloids and Surfaces A: Physicochem. Eng. Aspects **384**, 653–660 (2011).
[23]J. P. Peraud and E. Lauga, "Geometry and wetting of capillary folding," Phys. Rev. E **89**(4), 043011 (2014).
[24]D. Baratian, A. Cavalli, D. van den Ende, and F. Mugele, "On the shape of a droplet in a wedge: New insight from electrowetting," Soft Matter **11**(39), 7717–7721 (2015).
[25]C. Luo, M. Xiang, and X. Heng, "A stable intermediate wetting state after a water drop contacts the bottom of a microchannel or is placed on a single corner," Langmuir **28**(25), 9554–9561 (2012).
[26]E. Reyssat, "Drops and bubbles in wedges," J. Fluid Mech. **748**, 641–662 (2014).
[27]L. Keiser, R. Herbaut, J. Bico, and E. Reyssat, "Washing wedges: Capillary instability in a gradient of confinement," J. Fluid Mech. **790**, 619–633 (2016).
[28]Y. Zheng, J. Cheng, C. Zhou, H. Xing, X. Wen, P. Pi, and S. Xu, "Droplet motion on a shape gradient surface," Langmuir **33**(17), 4172–4177 (2017).
[29]X. Heng and C. Luo, "Liquid drop runs upward between two nonparallel plates," Langmuir **31**(9), 2743–2748 (2015).
[30]Y. Huang, L. Hu, W. Chen, X. Fu, X. Ruan, and H. Xie, "Directional transport of a liquid drop between parallel-nonparallel combinative plates," Langmuir **34**(15), 4484–4493 (2018).
[31]M. Ataei, T. Tang, and A. Amirfazli, "Motion of a liquid bridge between nonparallel surfaces," J Colloid Interface Sci. **492**, 218–228 (2017).
[32]M. Ataei, H. Chen, and A. Amirfazli, "Behavior of a liquid bridge between nonparallel hydrophobic surfaces," Langmuir **33**(51), 14674–14683 (2017).
[33]C. Luo, X. Heng, and M. Xiang, "Behavior of a liquid drop between two nonparallel plates," Langmuir **30**(28), 8373–8830 (2014).
[34]M. Prakash, D. Quere, and J. W. Bush, "Surface tension transport of prey by feeding shorebirds: The capillary ratchet," Science **320**, 931–934 (2008).
[35]C. Luo and X. Heng, "Separation of oil from a water/oil mixed drop using two nonparallel plates," Langmuir **30**(33), 10002–10010 (2014).
[36]W. Xu, Z. Lan, B. Peng, R. Wen, Y. Chen, and X. Ma, "Directional movement of droplets in grooves: suspended or immersed?," Sci. Rep. **6**, 18836 (2016).
[37]D. Langbein, "The shape and stability of liquid menisci at solid edges," J. Fluid Mech. **213**, 251–265 (1990).
[38]K. Khare, M. Brinkmann, B. M. Law, E. L. Gurevich, S. Herminghaus, and R. Seemann, "Dewetting of liquid filaments in wedge-shaped grooves," Langmuir **23**, 12138–12141 (2007).
[39]M. Kitron-Belinkov, A. Marmur, T. Trabold, and G. V. Dadheech, "Groovy drops: Effect of groove curvature on spontaneous capillary flow," Langmuir **23**(16), 8406–8410 (2007).
[40]P. Kant, A. L. Hazel, M. Dowling, A. B. Thompson, and A. Juel, "Controlling droplet spreading with topography," Phys. Rev. Fluids **2**, 094002 (2017).
[41]A. Giacomello, M. Chinappi, S. Meloni, and C. M. Casciola, "Metastable wetting on superhydrophobic surfaces: continuum and atomistic views of the Cassie-Baxter-Wenzel transition," Phys. Rev. Lett. **109**(22), 226102 (2012).
[42]N. Savva, S. Kalliadasis, and G. A. Pavliotis, "Two-dimensional droplet spreading over random topographical substrates," Phys. Rev. Lett. **104**(8), 084501 (2010).